

The Rotator Cable Does Not Stress Shield the Crescent Area During Shoulder Abduction

Christopher C. Schmidt, MD, Christopher S. Spicer, MS, Dimitrios V. Papadopoulos, MD, Sean M. Delserro, MME, Yoshiaki Tomizuka, MD, Thomas R. Zink, DO, Ryan J. Blake, MME, Michael P. Smolinski, MME, Mark Carl Miller, PhD, James M. Greenwell, BS, Luis F. Carrazana-Suarez, MD, and Patrick J. Smolinski, PhD

Investigation performed at the Shoulder and Elbow Mechanical Research Laboratory, Department of Orthopaedic Surgery, University of Pittsburgh Medical Center, Pittsburgh, Pennsylvania

Background: It is accepted by the orthopaedic community that the rotator cable (RCa) acts as a suspension bridge that stress shields the crescent area (CA). The goal of this study was to determine if the RCa does stress shield the CA during shoulder abduction.

Methods: The principal strain magnitude and direction in the RCa and CA and shoulder abduction force were measured in 20 cadaveric specimens. Ten specimens underwent a release of the anterior cable insertion followed by a posterior release. In the other 10, a release of the posterior cable insertion was followed by an anterior release. Testing was performed for the native, single-release, and full-release conditions. The thicknesses of the RCa and CA were measured.

Results: Neither the principal strain magnitude nor the strain direction in either the RCa or the CA changed with single or full RCa release ($p \geq 0.493$). There were no changes in abduction force after single or full RCa release ($p \geq 0.180$). The RCa and CA thicknesses did not differ from one another at any location ($p \geq 0.195$).

Conclusions: The RCa does not act as a suspension bridge and does not stress shield the CA. The CA primarily transfers shoulder abduction force to the greater tuberosity.

Clinical Relevance: The CA is important in force transmission during shoulder abduction, and efforts should be made to restore its continuity with a repair or reconstruction.

The rotator cable (RCa) is a semilunar band of collagen fibers surrounding the lateral supraspinatus and infraspinatus tendons, called the *crescent area* (CA), and is reportedly 2 to 3 times thicker than the CA (Fig. 1-A)¹. It runs perpendicular to the longitudinal fibers of the rotator cuff tendons and attaches to the humerus anteriorly via the coracohumeral ligament and posteriorly between the infraspinatus and teres minor humeral footprints (Figs. 1-B and 1-C)^{1,2}. Because of its thickness and unique anatomy, the RCa is thought to stress shield the CA by transmitting the rotator cuff contractile force around the CA to its humeral insertions, similar to a suspension bridge cable^{1,3}.

Our current understanding of rotator cuff force transmission pivots around the concept that the RCa shields the CA from stress by being the main conduit for abduction force^{1,4,5}. Despite the accepted importance of the RCa, there are studies supporting and refuting its mechanical role⁶⁻¹². Mesiha et al. supported the sus-

pension bridge concept by showing that an anterior cable release, compared with a crescent release, resulted in increased strain in the CA⁹. In that study, the increased strain was used to confirm the concept of the RCa stress shielding the CA⁹. Wang et al. questioned the role of the RCa as an important structure by demonstrating that an entire RCa release, compared with the unreleased condition, resulted in no increase in the middle deltoid force required for 60° of dynamic shoulder abduction¹².

The goal of this study was to measure strain magnitude and direction in the CA following RCa releases to determine whether the RCa stress shields the CA during shoulder abduction. CA strain is a measure of CA stress when assessed within a specimen at the same location^{1,9}. We hypothesized that RCa releases would increase the CA's strain magnitude and alter its strain direction. Furthermore, we hypothesized that RCa releases would decrease the shoulder abduction force and that the RCa is thicker than the CA¹.

Disclosure: The **Disclosure of Potential Conflicts of Interest** forms are provided with the online version of the article (<http://links.lww.com/JBJS/H39>).

Copyright © 2022 The Authors. Published by The Journal of Bone and Joint Surgery, Incorporated. All rights reserved. This is an open-access article distributed under the terms of the [Creative Commons Attribution-Non Commercial-No Derivatives License 4.0](https://creativecommons.org/licenses/by-nc-nd/4.0/) (CCBY-NC-ND), where it is permissible to download and share the work provided it is properly cited. The work cannot be changed in any way or used commercially without permission from the journal.

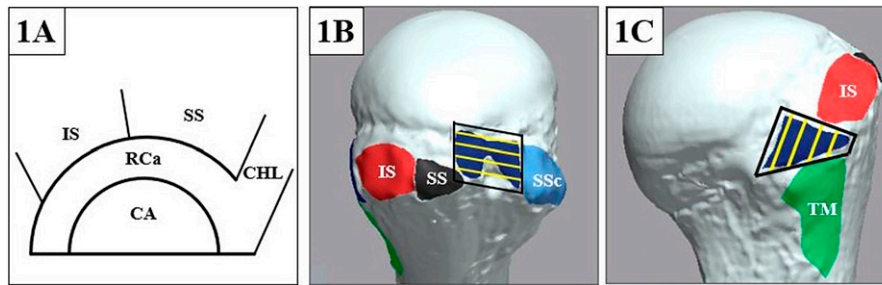


Fig. 1
Fig. 1-A A schematic of the supraspinatus (SS) and infraspinatus (IS) tendinous capsular complex showing the spatial relationships among the rotator cable (RCa), crescent area (CA), coracohumeral ligament (CHL), supraspinatus tendon (SS), and infraspinatus tendon (IS). The RCa inserts into the anterior aspect of the humerus through the coracohumeral ligament, between the supraspinatus and subscapularis tendons. (Reprinted, with modification, from: Zink TR, Schmidt CC, Papadopoulos DV, Blake RJ, Smolinski MP, Davidson AJ, Spicer CS, Miller MC, Smolinski PJ. Locating the rotator cable during subacromial arthroscopy: bursal- and articular-sided anatomy. *J Shoulder Elbow Surg.* 2021 Jul;30[7S]:S57-65. Reproduced with permission conveyed through Copyright Clearance Center, Inc.) **Fig. 1-B** A 3D model of the anterior RCa footprint, shaded in dark blue and outlined by the black box. The anterior part of the RCa attaches to the humerus through the coracohumeral ligament (dark blue area), which attaches to the humerus around the bicipital groove. The horizontal yellow lines illustrate the area cut off the humerus during an anterior RCa release. SSc = subscapularis. **Fig. 1-C** A 3D model of the posterior RCa footprint, shaded in dark blue and outlined by the black trapezoid. The posterior part of the RCa attaches to the humerus between the infraspinatus (IS) and teres minor (TM) footprints. The vertical yellow lines illustrate the area cut off the humerus during a posterior RCa release.

Materials and Methods

Experimental Design

Twenty fresh-frozen human cadaveric specimens were secured into a shoulder simulator, and the rotator cuff muscles were loaded with physiological forces. The mechanical tests measured strain magnitude and direction in the RCa and CA and shoulder abduction force. The measurements were made in 0° and 30° of abduction in the scapular plane, where the supraspinatus is the main shoulder abductor¹³⁻¹⁵. After baseline testing, 10 specimens underwent an anterior-first RCa release followed by a full RCa release. In the other 10

specimens, a posterior-first RCa release was followed by a full RCa release. Anterior- or posterior-first procedures were randomized using Excel (Microsoft). Mechanical testing of each specimen was performed for the native (unreleased), single-release, and full-release conditions. The thicknesses of the RCa and CA were measured using a laser micrometer (FaroArm; FARO).

Specimen Preparation

Thirty-four fresh-frozen cadaveric arms, from the scapula to the fingertips, were procured for this study. Exclusion criteria

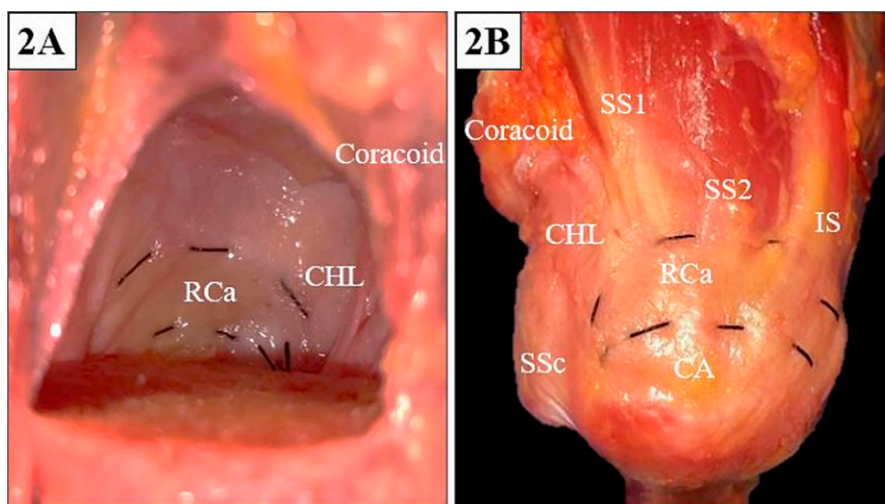


Fig. 2
Fig. 2-A A photograph showing the rotator cable (RCa) outlined by suture from the articular side. An inferior capsulotomy and humeral osteotomy were performed to expose the RCa, seen only from the articular side. The rotator cuff capsular complex remains intact. **Fig. 2-B** The RCa is marked by suture from the bursal side. SSc = subscapularis; CHL = coracohumeral ligament; SS1 = anterior cord of the SS tendon; SS2 = posterior half of the supraspinatus tendon, which is strap-like; CA = crescent area; and IS = infraspinatus.

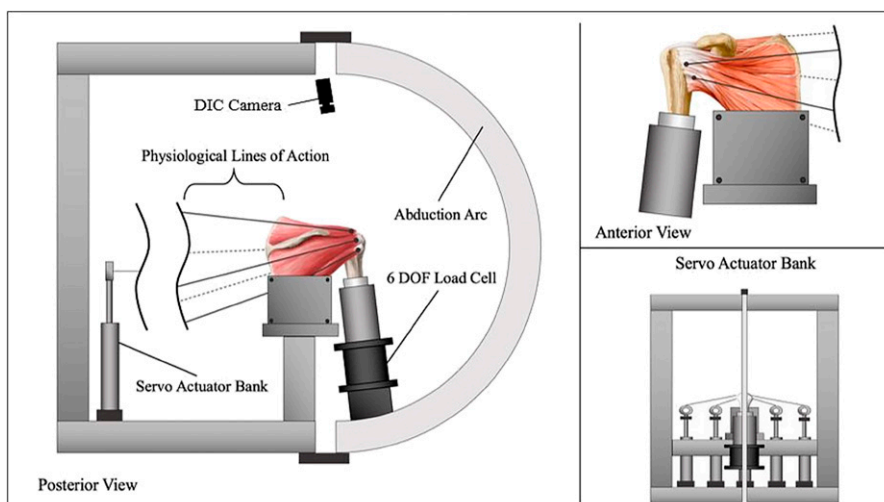


Fig. 3
A schematic of the shoulder simulator.

were a partial- or full-thickness rotator cuff tear or shoulder arthritis. Twenty specimens (mean age and standard deviation at the time of death, 67 ± 17 years) met the above criteria. The humeri were cut 5 cm distal to the deltoid insertion. The soft tissue and clavicle were excised from each specimen to the level of the rotator cuff/capsular structures. An acromionectomy was performed to visualize the rotator cuff. An anatomic neck osteotomy was done to remove the humeral head and expose the RCa. During the humeral osteotomy, the attachments of the rotator cuff-cable complex were carefully preserved. The RCa was outlined with a running silk suture (Figs. 2-A and 2-B). After the RCa was marked, the humeral head was reduced and was fixed with 2 screws. A preliminary study comparing no osteotomy to a repaired humeral osteotomy found no statistical difference in either strain magnitude ($p \geq 0.746$) or shoulder abduction force ($p \geq 0.231$) (see Appendices I and II). Locking,

heavy number-2 braided sutures were sewn into each rotator cuff tendon (supraspinatus, infraspinatus, teres minor, and upper and lower subscapularis). Eyelet screws were fixed to the scapula along the anatomic lines of pull for connection of the sutures with the loading cables. The specimen was secured to the simulator by fixing the scapula and humerus to custom-built fixtures using bolts and polyester resin (Bondo; 3M).

Shoulder Simulator

The validated shoulder simulator consists of an aluminum frame and 5 servo-driven actuators (Parker Hannifin) (Fig. 3). Muscles lines of action were simulated by cables running through pulleys that connected to a single-DOF (degree-of-freedom) load cell (MLP-100; Transducer Techniques) (accuracy $\pm 0.25\%$ rated output [RO]), non-repeatability = 0.05% RO) on each actuator. The actuators operated using force feedback control (LabVIEW;

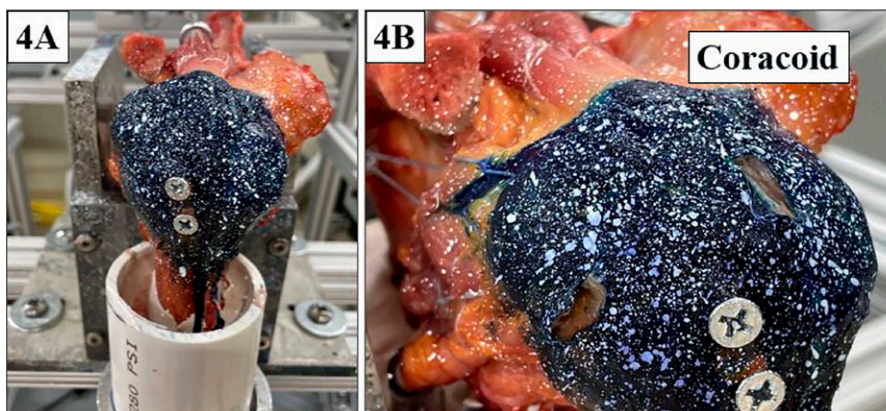


Fig. 4
A specimen stained with methylene blue and randomly speckled with white ink before release (Fig. 4-A) and after both anterior and posterior RCa releases—i.e., a full release (Fig. 4-B). The anterior release is done by completely sectioning the attached tissue off the humerus between the anterior supraspinatus and superior supraspinatus footprints (i.e., at the coracohumeral ligament). The posterior release is done by sectioning the attached tissue between the infraspinatus and teres minor footprints.

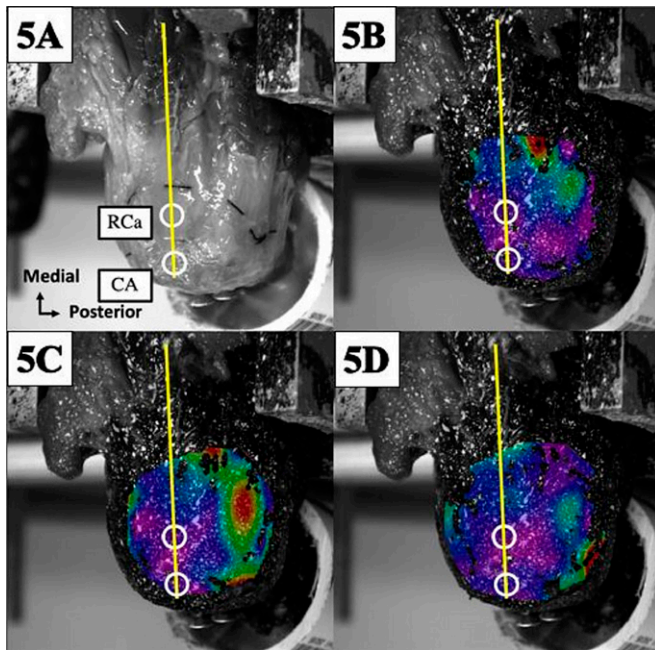


Fig. 5

Fig. 5-A A photograph of the rotator cable (RCa) and crescent area (CA) in their native condition was obtained to ensure accuracy and reproducibility of the measurement area. The principal strain in the RCa and CA was measured on the supraspinatus bisecting line. The RCa area that was analyzed was in the center of the cable, whereas the CA was sampled one-half cable width lateral to the RCa area. DIC strain images were obtained of a native specimen (**Fig. 5-B**), after anterior-first release (**Fig. 5-C**), and after full release (**Fig. 5-D**). Note that the coloring does not change with anterior or full RCa release, a qualitative finding indicating that CA strain is not dependent on the RCa condition.

National Instruments). A custom arc was used to set abduction angles, and the scapular retention fixture was bolted to the simulator such that the glenohumeral joint was centered in the abduction arc. The fixture holding the distal part of the humerus was attached to a 6-DOF load cell (Bertec) (accuracy ± 0.1 N) to measure shoulder abduction force. The load cell had 3 axes of measurement, with 1 axis aligned with scaption to directly record abduction force.

A 2-camera digital image correlation (DIC) system (Vic-3D; Correlated Solutions) (high strain resolution ± 10 μ m, in-plane resolution = $1/200,000 \times$ FOV [field of view]) was mounted to the simulator frame above the humeral head of each specimen so that the entire RCa was visible to both cameras. The system was calibrated for each specimen (Fig. 3). The DIC system measures tissue principal strain magnitude and direction, the former of which was defined as the maximal strain where shear strain equaled zero.

Mechanical Testing

With the specimens mounted in the simulator, photographs were made of the native condition at both abduction angles; these images identified circular areas in the RCa and CA used

during principal strain measurements. The specimens were then stained with methylene blue followed by white ink randomly speckled over the dyed tissue to ensure a trackable pattern for the DIC (Fig. 4-A)^{16,17}.

The mechanical protocol centered the humeral head in the glenoid by incrementally loading each of the 5 rotator cuff tendons to 10 N. The 10-N preload on all muscles was maintained for 5 minutes. Testing was initiated by linearly ramping the load on the rotator cuff muscles to their predetermined physiological load and holding it constant for 1 minute. Physiological loads (supraspinatus = 80 N, infraspinatus = 90 N, teres minor = 97 N, upper supraspinatus = 108 N, and lower supraspinatus = 127 N) were based on muscle cross-sectional area and electromyographic activity^{18,19}. C-arm imaging after preload and during testing confirmed a centered glenohumeral joint.

The DIC system recorded images at 10 Hz for measuring tissue principal strain in the RCa and CA. Shoulder abduction force was measured at the unconstrained distal part of the humerus using the 6-DOF load cell, with values recorded by a data acquisition system (National Instruments).

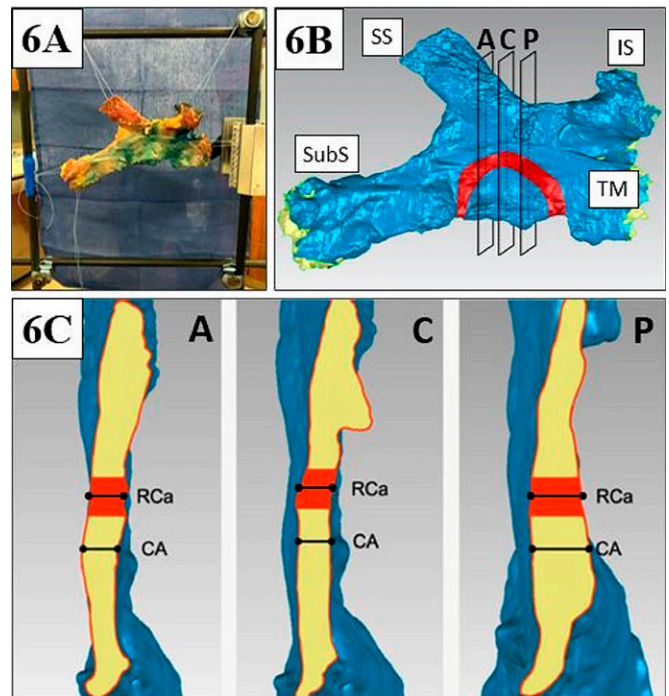


Fig. 6

Method of thickness measurement of the rotator cable (RCa) and crescent area (CA). **Fig. 6-A** To create accurate 3D models of the RCa and CA, the rotator cuff capsular complex was secured to a custom frame. **Fig. 6-B** A 3D model of the rotator cuff capsular complex showing that the RCa and CA were measured in 3 evenly distributed coronal planes. SS = supraspinatus, IS = infraspinatus, SubS = subscapularis, and TM = teres minor. **Fig. 6-C** Coronal sections (A = anterior, C = center, and P = posterior) of the rotator cuff capsular complex showing that the RCa thickness was measured at its mid-point and the CA was quantified 3 mm lateral to the lateral border of the RCa.

TABLE I Principal Strain Magnitude in the RCa and CA

Release/Abduction Angle	RCa State	Mean Strain (Std. Dev.) (mm/mm)	
		RCa	CA
Anterior-first*			
0°	Native	0.021 (0.014)	0.014 (0.009)
0°	Single release	0.027 (0.019)	0.018 (0.011)
0°	Full release	0.023 (0.012)	0.012 (0.005)
30°	Native	0.023 (0.012)	0.017 (0.010)
30°	Single release	0.020 (0.007)	0.015 (0.009)
30°	Full release	0.029 (0.021)	0.016 (0.012)
Posterior-first†			
0°	Native	0.020 (0.009)	0.015 (0.007)
0°	Single release	0.030 (0.026)	0.019 (0.015)
0°	Full release	0.026 (0.019)	0.016 (0.010)
30°	Native	0.036 (0.030)	0.020 (0.015)
30°	Single release	0.030 (0.021)	0.018 (0.012)
30°	Full release	0.033 (0.016)	0.018 (0.012)

*ANOVA p values for association of strain magnitude with cable release = 0.740, with abduction angle = 0.781, and with strain location = 0.024.
†ANOVA p values for association of strain magnitude with cable release = 0.772, with abduction angle = 0.319, and with strain location = 0.006.

After testing of the native condition, a randomized anterior- or posterior-first RCa release was performed and the specimen was retested. The anterior release was performed by cutting the coraco-

humeral ligament off its humeral footprint. The coracohumeral ligament is the anatomic structure recognized as the anterior insertion of the RCa (Fig. 1-B)^{1,2}. Other investigators have included the anterior cord of the supraspinatus tendon with the coracohumeral ligament when performing an anterior RCa release⁹. The anterior cord of the supraspinatus tendon is labeled SS1 in Figure 2-B. The posterior release was done by cutting off the rotator cuff capsular tissue between the infraspinatus and teres minor from the humerus (Fig. 1-C). After the single release, the opposite side was released—i.e., a full release was performed (Fig. 4-B). Testing was then carried out a third time. The testing for all 3 conditions (native, single release, and full release) was performed in a single session.

TABLE II Principal Strain Direction in the RCa and CA

Release/Abduction Angle	RCa State	Mean Strain Direction (Std. Dev.) (°)	
		RCa	CA
Anterior-first*			
0°	Native	181 (74.7)	192 (55.8)
0°	Single release	218 (40.3)	220 (36.2)
0°	Full release	230 (38.7)	228 (39.1)
30°	Native	212 (65.1)	215 (39.9)
30°	Single release	226 (49.2)	197 (61.2)
30°	Full release	194 (67.9)	188 (60.1)
Posterior-first†			
0°	Native	205 (53.5)	205 (52.8)
0°	Single release	200 (47.7)	204 (51.6)
0°	Full release	200 (51.3)	194 (51.2)
30°	Native	216 (47.6)	207 (72.7)
30°	Single release	204 (67.3)	228 (47.9)
30°	Full release	211 (58.1)	211 (60.0)

*ANOVA p values for association of strain direction with cable release = 0.493, with abduction angle = 0.580, and with strain location = 0.755. †ANOVA p values for association of strain direction with cable release = 0.925, with abduction angle = 0.295, and with strain location = 0.841.

Post-DIC Image Processing to Measure Principal Strain

The principal strain magnitude and direction were calculated in a circular area (radius = 2 mm) for both the RCa and the CA using DIC (Vic-3D) software. The locations were kept constant by positioning both circles on a line bisecting the supraspinatus muscle. The RCa circular area was centered between the 2 sutures outlining the cable, while the CA circular area was positioned one-half cable width lateral to the outside border of the RCa^{1,20}. The native-condition photograph (Fig. 5-A) was used as an onlay to ensure accuracy and reproducibility of the measurement area (Figs. 5-B, 5-C, and 5-D).

RCa and CA Thickness and Descriptive Parameters

After mechanical testing, the rotator cuff tendinous capsular complex was secured on a frame (Fig. 6-A). The RCa and CA thicknesses and descriptive parameters were measured using a laser micrometer (FaroArm). Three-dimensional solid models

TABLE III Shoulder Abduction Force

Release/Abduction Angle	RCa State	Mean Abduction Force (Std. Dev.) (N)
Anterior-first*		
0°	Native	22.4 (10.0)
0°	Single release	27.6 (8.1)
0°	Full release	30.4 (9.9)
30°	Native	9.1 (3.7)
30°	Single release	8.5 (4.2)
30°	Full release	10.0 (3.1)
Posterior-first†		
0°	Native	13.1 (8.9)
0°	Single release	15.7 (10.7)
0°	Full release	17.1 (10.5)
30°	Native	7.2 (2.3)
30°	Single release	6.6 (3.1)
30°	Full release	6.6 (2.9)

*ANOVA p values for association of abduction force with cable release = 0.180 and with abduction angle = <0.001. †ANOVA p values for association of abduction force with cable release = 0.777 and with abduction angle = <0.001.

were generated from laser scans using modeling software (Geomagic; 3D Systems) (Fig. 6-B). The RCa and CA thicknesses were measured in 3 evenly spaced coronal planes (anterior, center, and posterior) at constant points within the planes (Fig. 6-C). The RCa thickness was quantified at its midpoint, and the CA was measured 3 mm lateral to the lateral border of the RCa. The CA anteroposterior diameter, CA mediolateral diameter, and RCa width were measured from the solid models. Previous data in our laboratory showed no statistical difference ($p \geq 0.169$) between laser micrometer and scientific caliper measurements (accuracy 0.01 mm, L.S. Starrett)²⁰.

Statistical Analysis

A priori sample size analysis was based on the finding that small rotator cable releases increased the CA strain significantly ($p < 0.05$), from 5% to 6%; this strain change was associated with a substantial decrease ($p = 0.024$) in tendon stiffness⁹. Six specimens were needed in each group to detect a 1% difference in strain with a statistical power of 0.95 (G*Power, University of Düsseldorf) (see Appendix III)⁹.

Principal strain and abduction force data were statistically analyzed by group based on anterior-first or posterior-first release. The principal strain magnitude and direction were determined by using a 3-factor analysis of variance (ANOVA) with the RCa state, abduction angle, and strain location as the factors. The analysis of the abduction force was performed using a 2-factor ANOVA with the RCa state and abduction angle as the factors. Thickness was analyzed using independent-sample t tests.

Source of Funding

No external funding was received for this study.

Results

Mechanical testing of 18 specimens was completed. Two specimens, 1 in each group, were excluded due to either infraspinatus tendon tearing or load cell malfunction.

Figures 5-B, 5-C, and 5-D are representative images depicting principal strain. The principal strain magnitude in the RCa or CA did not change ($p \geq 0.319$) with either anterior-first release, posterior-first release, or full release in either of the 2 abduction positions (Table I). Independent of the testing condition, principal strain remained significantly greater in the RCa than in the CA ($p \leq 0.024$). The principal strain direction was not dependent on the RCa release state, abduction angle, or strain location ($p \geq 0.295$) (Table II).

There were no significant changes in abduction force among the anterior-first, posterior-first, and full-release conditions ($p \geq 0.180$) (Table III).

The average thicknesses of the RCa (6.5 ± 2.1 mm) and CA (5.9 ± 2.0 mm) were not statistically different from one another ($p = 0.422$) or at any of the 3 single measurement locations ($p \geq 0.195$) (Table IV). Figure 7 shows the descriptive anatomy of the CA and RCa, with raw data shown in Appendices IV through VIII.

Discussion

This study shows that the RCa does not stress shield the CA during shoulder abduction. Partial or full RCa releases did not change the principal strain magnitude ($p \geq 0.740$) or direction ($p \geq 0.493$). The above tissue strains indicate that the RCa does not stress shield the CA because CA strain acted as a measure of CA stress in the present study. In other words, the CA strain was independent of the condition of the RCa. Furthermore, the RCa thickness of 6.5 mm was similar to the CA thickness of 5.9 mm ($p = 0.422$), indicating that the RCa does not adaptively thicken with age as a result of its perceived role as a suspension bridge cable¹³. The absence of RCa strain shielding helps to clarify why, in the clinical setting, RCa-intact and RCa-disrupted rotator cuff tears enlarge at similar rates²¹.

Surprisingly, there were no significant changes in shoulder abduction force between the single- and full-RCa release conditions ($p \geq 0.180$). The above results, together with previous literature showing a substantial reduction of abduction force

TABLE IV RCa and CA Thicknesses by Location

	Anterior	Center	Posterior	Combined
Mean thickness (std. dev.)				
RCa	6.4 (2.5)	6.2 (2.1)	6.9 (2.4)	6.5 (2.1)
CA	5.4 (2.0)	5.7 (2.1)	6.8 (2.6)	5.9 (2.0)
P value	0.195	0.469	0.881	0.422

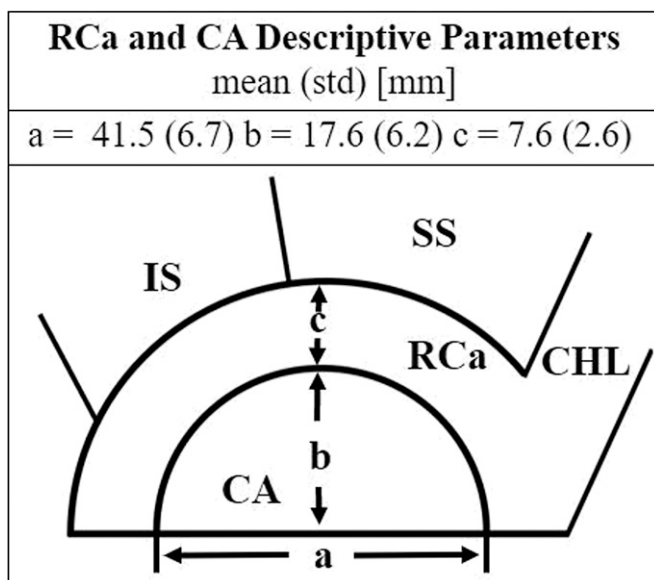


Fig. 7
Schematic of the rotator cable (RCa) and crescent area (CA) descriptive parameters. a = CA anteroposterior diameter, b = CA mediolateral diameter, c = RCa width, SS = supraspinatus, IS = infraspinatus, and CHL = coracohumeral ligament.

with a partially released CA and an intact RCa^{8,22}, strongly suggest that the shoulder abduction force is transmitted primarily through the CA and not the RCa. An intact CA seems to be a mechanical prerequisite for return of clinical abduction strength. The CA's mechanical role in force transmission explains why shoulder abduction strength is greater when supraspinatus and infraspinatus tendon repairs heal versus when they do not heal²³⁻²⁶. Furthermore, a comparison of

posterosuperior irreparable rotator cuff tears treated with CA reconstruction versus no reconstruction demonstrated a clinically important increase in shoulder abduction strength ($p < 0.001$)²⁷.

A biomechanical study simulating RCa and CA tears by Mesiha et al. showed that, compared with CA tears, RCa tears lead to a greater tear gap distance ($p = 0.002$), a greater decrease in tendon stiffness ($p = 0.002$), and an asymmetric regional strain pattern ($p < 0.05$)⁹. Those findings favor the hypothesis that there is RCa stress shielding of the CA; however, the simulated RCa releases in that study differed from those in the present study and the anatomic literature^{1,2,9,20}. Mesiha et al. not only released the coracohumeral ligament but included the anterior cord of the supraspinatus tendon (Fig. 8-A)^{9,28-30}. The fibers of the RCa insert anteriorly into the humerus through the coracohumeral ligament and not the anterior cord of the supraspinatus tendon (Fig. 8-B)^{1,2,20}. Furthermore, Mesiha et al. reported an average CA anteroposterior diameter of 13 mm (range, 10 to 17 mm)⁹, which is smaller than the average value of 42 mm (range, 33 to 53 mm) in the present study and of 41 mm (range, 31 to 52 mm) in a study by Burkhart et al.¹. The smaller CA anteroposterior diameter reported by Mesiha et al.⁹ supports the premise that the anterior cord of the supraspinatus tendon and the coracohumeral ligament were both sectioned in their study. In the current study, the anterior cord of the supraspinatus tendon was preserved.

Repairing the RCa's humeral attachments during a partial or full repair of a massive rotator cuff tear is reported to be an important step in reversing pseudoparalysis^{3,8,31-37}. However, what if in reversing pseudoparalysis it is not the RCa acting as a bridge cable, but rather the lower supraspinatus and teres minor muscles stabilizing the humerus in the glenoid (concavity-compression)^{12,38-40}? The strain findings of our study show that the

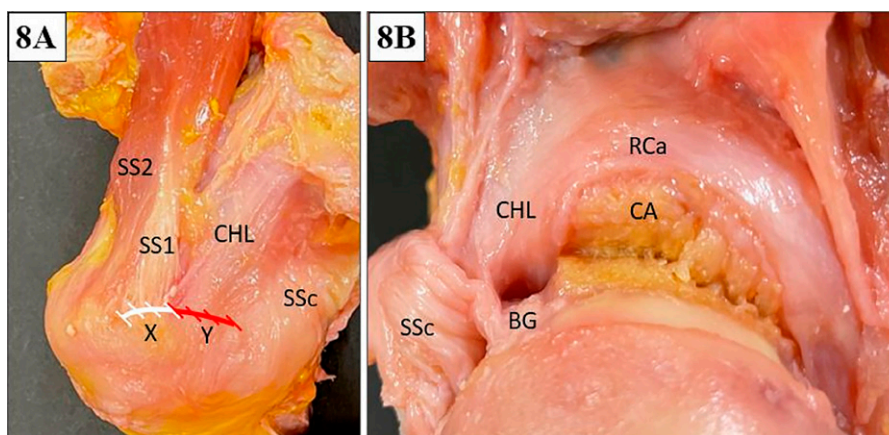


Fig. 8
Fig. 8-A In the study by Mesiha et al.⁹, the anterior rotator cable (RCa) release started posterior to the anterior cord of the supraspinatus tendon (SS1) as shown by the white hashed line (X), whereas in the present study the anterior RCa release started anterior to the anterior cord of the supraspinatus tendon (SS1) as illustrated by the red hashed line (Y). SS2 = strap-like posterior part of the supraspinatus tendon, SS1 = cord-like anterior part of the supraspinatus tendon, CHL = coracohumeral ligament, and SS3 = subscapularis. **Fig. 8-B** Articular side of the rotator cuff capsular complex showing that the RCa inserts into the anterior aspect of the humerus through the coracohumeral ligament (CHL). This specimen was excluded from mechanical testing because it has a partial-thickness tear of the supraspinatus and infraspinatus tendons. BG = bicipital groove and CA = crescent area.

RCa does not act as a bridge cable carrying muscle forces around the CA. Clinical and mechanical studies suggest that the presence or absence of pseudoparalysis is determined by the tear pattern and size, not the state of the RCa^{12,32,41,42}. A recent dynamic shoulder model showed that anterior, middle, or full release of the RCa had no statistical ($p < 0.05$) effect on subacromial contact pressure, area, or force during shoulder abduction, indicating no superior humeral head migration¹². However, humeral head migration did occur with complete release of the entire anteroposterior cuff above the humeral equator. Those findings support the concept that functioning lower supraspinatus and teres minor muscles are needed to prevent pseudoparalysis¹².

The thicknesses of the RCa and CA were not significantly different from one another in any of 3 measured locations ($p \geq 0.195$). The average thickness was 6.5 ± 2.1 mm for the RCa and 5.9 ± 2.0 mm for the CA. Our thickness findings differ from published values of 4.72 mm for the RCa and 1.82 mm for the CA¹. It is difficult to explain the variation in thickness between the 2 studies because the measurements were taken at similar locations with comparable techniques on relatively the same number of specimens from similarly aged donors^{1,20}. It is possible that differences in specimen dissection methods, tissue hydration, and position at the time of measurement may account for the discrepancy.

The principal strain magnitude in the RCa throughout the testing conditions was always greater than that in the CA ($p \leq 0.024$). At first glance, the larger strain in the RCa relative to the CA supports the suspension bridge hypothesis. However, neither the principal strain magnitude nor its direction changed with partial or full releases ($p \geq 0.493$). These higher strains in the RCa are due to the differences in material properties, tissue composition, and fiber direction, not higher stresses^{2,6,43,44}. Also, the shoulder abduction force was larger at 0° than 30° of scaption ($p < 0.001$); we believe that this is due to the weight of the arm.

The limitations of this study are that tissue strain and abduction force were measured in 0° and 30° of abduction without a deltoid force^{11,13}. Nevertheless, simplifying the study design limited confounding variables^{9,45}. The findings may not apply to other arm positions or loading conditions. However, other isometric mechanical studies of rotator cuffs tested at similar abduction angles explain and predict clinical observations^{4,8,9,45,46}. The anterior part of the RCa may not have been fully released due to crossing fibers into the subscapularis⁴⁷; however, a mechanical effect was not reported even with an entire RCa release¹². The strengths of the study are the physiological loading, the large number of specimens, knowledge of the

RCa location, and noncontact methods for quantifying strain and thickness.

In conclusion, releasing the RCa did not affect the CA strain vector or shoulder abduction force. Contrary to the prevailing thoughts on the mechanical importance of the RCa, our findings indicate that the RCa does not need to be repaired or reconstructed to improve shoulder abduction strength. The RCa does not act as a suspension bridge cable. The CA is important in supraspinatus and infraspinatus force transmission^{8,22} and, when torn, surgical efforts should be made to restore its integrity.

Appendix

eA Supporting material provided by the authors is posted with the online version of this article as a data supplement at [jbjs.org \(http://links.lww.com/JBJS/H40\)](http://links.lww.com/JBJS/H40). ■

NOTE: The authors acknowledge Sean Cooke, BS, Department of Orthopaedic Surgery and Shoulder and Elbow Mechanical Research Laboratory, University of Pittsburgh Medical Center, for manuscript editing and formatting.

Christopher C. Schmidt, MD^{1,2,3}
Christopher S. Spicer, MS^{2,3}
Dimitrios V. Papadopoulos, MD^{1,2}
Sean M. Delserso, MME^{2,3}
Yoshiaki Tomizuka, MD^{1,2,4}
Thomas R. Zink, DO^{1,2}
Ryan J. Blake, MME^{2,3}
Michael P. Smolinski, MME^{2,3}
Mark Carl Miller, PhD^{2,3}
James M. Greenwell, BS²
Luis F. Carrazana-Suarez, MD^{1,2}
Patrick J. Smolinski, PhD^{2,3}

¹Department of Orthopaedic Surgery, University of Pittsburgh Medical Center, Pittsburgh, Pennsylvania

²Shoulder and Elbow Mechanical Research Laboratory, Department of Orthopaedic Surgery, University of Pittsburgh Medical Center, Pittsburgh, Pennsylvania

³Department of Mechanical Engineering and Material Science, University of Pittsburgh, Pittsburgh, Pennsylvania

⁴Department of Orthopaedic Surgery, Nihon University School of Medicine, Tokyo, Japan

Email for corresponding author: schmidtc@upmc.edu

References

- Burkhart SS, Esch JC, Jolson RS. The rotator crescent and rotator cable: an anatomic description of the shoulder's "suspension bridge". *Arthroscopy*. 1993; 9(6):611-6.
- Clark JM, Harryman DT 2nd. Tendons, ligaments, and capsule of the rotator cuff. Gross and microscopic anatomy. *J Bone Joint Surg Am*. 1992 Jun;74(5):713-25.
- Burkhart SS. Fluoroscopic comparison of kinematic patterns in massive rotator cuff tears. A suspension bridge model. *Clin Orthop Relat Res*. 1992 Nov;(284):144-52.
- Duralde XA. How important is the anterior rotator cuff cable?: commentary on an article by Mena M. Mesiha, MD, et al.: "The biomechanical relevance of anterior rotator cuff cable tears in a cadaveric shoulder model". *J Bone Joint Surg Am*. 2013 Oct 16;95(20):e156.
- Petersen W. Re: The rotator crescent and rotator cable: an anatomic description of the shoulder's "suspension bridge". *Arthroscopy*. 2010 Feb;26(2):256-7.
- Arai R, Matsuda S. Macroscopic and microscopic anatomy of the rotator cable in the shoulder. *J Orthop Sci*. 2020 Mar;25(2):229-34.
- Davis DE, Lee B, Aleem A, Abboud J, Ramsey M. Interobserver reliability of the rotator cable and its relationship to rotator cuff congruity. *J Shoulder Elbow Surg*. 2020 Sep;29(9):1811-4.

8. Halder AM, O'Driscoll SW, Heers G, Mura N, Zobitz ME, An KN, Kreuzsch-Brinker R. Biomechanical comparison of effects of supraspinatus tendon detachments, tendon defects, and muscle retractions. *J Bone Joint Surg Am*. 2002 May;84(5):780-5.
9. Mesiha MM, Derwin KA, Sibole SC, Erdemir A, McCarron JA. The biomechanical relevance of anterior rotator cuff cable tears in a cadaveric shoulder model. *J Bone Joint Surg Am*. 2013 Oct 16;95(20):1817-24.
10. Nguyen ML, Quigley RJ, Galle SE, McGarry MH, Jun BJ, Gupta R, Burkhart SS, Lee TQ. Margin convergence anchorage to bone for reconstruction of the anterior attachment of the rotator cable. *Arthroscopy*. 2012 Sep;28(9):1237-45.
11. Oh JH, Jun BJ, McGarry MH, Lee TQ. Does a critical rotator cuff tear stage exist?: a biomechanical study of rotator cuff tear progression in human cadaver shoulders. *J Bone Joint Surg Am*. 2011 Nov 16;93(22):2100-9.
12. Wang L, Kang Y, Xie G, Cai J, Chen C, Yan X, Jiang J, Zhao J. Incomplete Rotator Cable Did Not Cause Rotator Cuff Dysfunction in Case of Rotator Cuff Tear: A Biomechanical Study of the Relationship Between Rotator Cable Integrity and Rotator Cuff Function. *Arthroscopy*. 2021 Aug;37(8):2444-51.
13. McMahon PJ, Debski RE, Thompson WO, Warner JJ, Fu FH, Woo SL. Shoulder muscle forces and tendon excursions during glenohumeral abduction in the scapular plane. *J Shoulder Elbow Surg*. 1995 May-Jun;4(3):199-208.
14. Alpert SW, Pink MM, Jobe FW, McMahon PJ, Mathiyakom W. Electromyographic analysis of deltoid and rotator cuff function under varying loads and speeds. *J Shoulder Elbow Surg*. 2000 Jan-Feb;9(1):47-58.
15. Thompson WO, Debski RE, Boardman ND 3rd, Taskiran E, Warner JJ, Fu FH, Woo SL. A biomechanical analysis of rotator cuff deficiency in a cadaveric model. *Am J Sports Med*. 1996 May-Jun;24(3):286-92.
16. Andarawis-Puri N, Ricchetti ET, Soslosky LJ. Rotator cuff tendon strain correlates with tear propagation. *J Biomech*. 2009 Jan 19;42(2):158-63.
17. Palanca M, Tozzi G, Critosfollini L. The use of digital image correlation in the biomechanical area: a review. *Int. Biomech*. 2016;3(1):1-21.
18. Kedgley AE, Mackenzie GA, Ferreira LM, Drosdowech DS, King GJ, Faber KJ, Johnson JA. The effect of muscle loading on the kinematics of in vitro glenohumeral abduction. *J Biomech*. 2007;40(13):2953-60.
19. Omi R, Sano H, Ohnuma M, Kishimoto KN, Watanuki S, Tashiro M, Itoi E. Function of the shoulder muscles during arm elevation: an assessment using positron emission tomography. *J Anat*. 2010 May;216(5):643-9.
20. Zink TR, Schmidt CC, Papadopoulos DV, Blake RJ, Smolinski MP, Davidson AJ, Spicer CS, Miller MC, Smolinski PJ. Locating the rotator cable during subacromial arthroscopy: bursal- and articular-sided anatomy. *J Shoulder Elbow Surg*. 2021 Jul;30(7S):S57-65.
21. Keener JD, Hsu JE, Steger-May K, Teefey SA, Chamberlain AM, Yamaguchi K. Patterns of tear progression for asymptomatic degenerative rotator cuff tears. *J Shoulder Elbow Surg*. 2015 Dec;24(12):1845-51.
22. Schmidt CC, Blake RJ, Carrazana-Suarez LF, Papadopoulos DV, Smolinski MP, Greenwell J, Cook AJ, Miller MC, Smolinski PJ. Effects of Rotator Cable and Crescent Area Tear Propagation on Humeral Abduction Strength. Presented as a poster exhibit at the Annual Meeting of the American Academy of Orthopaedic Surgeons; 2022 Mar 22-23; Chicago, IL. Poster no. P0288.
23. Cole BJ, McCarty LP 3rd, Kang RW, Alford W, Lewis PB, Hayden JK. Arthroscopic rotator cuff repair: prospective functional outcome and repair integrity at minimum 2-year follow-up. *J Shoulder Elbow Surg*. 2007 Sep-Oct;16(5):579-85.
24. Harryman DT 2nd, Mack LA, Wang KY, Jackins SE, Richardson ML, Matsen FA 3rd. Repairs of the rotator cuff. Correlation of functional results with integrity of the cuff. *J Bone Joint Surg Am*. 1991 Aug;73(7):982-9.
25. Iannotti JP, Deutsch A, Green A, Rudicel S, Christensen J, Marraffino S, Rodeo S. Time to failure after rotator cuff repair: a prospective imaging study. *J Bone Joint Surg Am*. 2013 Jun 5;95(11):965-71.
26. Lapner PL, Sabri E, Rakhra K, McRae S, Leiter J, Bell K, Macdonald P. A multicenter randomized controlled trial comparing single-row with double-row fixation in arthroscopic rotator cuff repair. *J Bone Joint Surg Am*. 2012 Jul 18;94(14):1249-57.
27. Mori D, Funakoshi N, Yamashita F. Arthroscopic surgery of irreparable large or massive rotator cuff tears with low-grade fatty degeneration of the infraspinatus: patch autograft procedure versus partial repair procedure. *Arthroscopy*. 2013 Dec;29(12):1911-21.
28. Mochizuki T, Sugaya H, Uomizu M, Maeda K, Matsuki K, Sekiya I, Muneta T, Akita K. Humeral insertion of the supraspinatus and infraspinatus. New anatomical findings regarding the footprint of the rotator cuff. *J Bone Joint Surg Am*. 2008 May;90(5):962-9.
29. Roh MS, Wang VM, April EW, Pollock RG, Bigliani LU, Flatow EL. Anterior and posterior musculotendinous anatomy of the supraspinatus. *J Shoulder Elbow Surg*. 2000 Sep-Oct;9(5):436-40.
30. Volk AG, Vangness CT Jr. An anatomic study of the supraspinatus muscle and tendon. *Clin Orthop Relat Res*. 2001 Mar;(384):280-5.
31. Burkhart SS, Nottage WM, Ogilvie-Harris DJ, Kohn HS, Pachelli A. Partial repair of irreparable rotator cuff tears. *Arthroscopy*. 1994 Aug;10(4):363-70.
32. Collin P, Matsumura N, Lädermann A, Denard PJ, Walch G. Relationship between massive chronic rotator cuff tear pattern and loss of active shoulder range of motion. *J Shoulder Elbow Surg*. 2014 Aug;23(8):1195-202.
33. Denard PJ, Koo SS, Murena L, Burkhart SS. Pseudoparalysis: the importance of rotator cable integrity. *Orthopedics*. 2012 Sep;35(9):e1353-7.
34. Kim SJ, Lee IS, Kim SH, Lee WY, Chun YM. Arthroscopic partial repair of irreparable large to massive rotator cuff tears. *Arthroscopy*. 2012 Jun;28(6):761-8.
35. Moser M, Jablonski MV, Horodyski M, Wright TW. Functional outcome of surgically treated massive rotator cuff tears: a comparison of complete repair, partial repair, and debridement. *Orthopedics*. 2007 Jun;30(6):479-82.
36. Porcellini G, Castagna A, Cesari E, Merolla G, Pellegrini A, Paladini P. Partial repair of irreparable supraspinatus tendon tears: clinical and radiographic evaluations at long-term follow-up. *J Shoulder Elbow Surg*. 2011 Oct;20(7):1170-7.
37. Wellmann M, Lichtenberg S, da Silva G, Magosch P, Habermeyer P. Results of arthroscopic partial repair of large retracted rotator cuff tears. *Arthroscopy*. 2013 Aug;29(8):1275-82.
38. Lippitt S, Matsen F. Mechanisms of glenohumeral joint stability. *Clin Orthop Relat Res*. 1993 Jun;(291):20-8.
39. Lippitt SB, Vanderhooff JE, Harris SL, Sidles JA, Harryman DT 2nd, Matsen FA 3rd. Glenohumeral stability from concavity-compression: A quantitative analysis. *J Shoulder Elbow Surg*. 1993 Jan;2(1):27-35.
40. Parsons IM, Apreleva M, Fu FH, Woo SL. The effect of rotator cuff tears on reaction forces at the glenohumeral joint. *J Orthop Res*. 2002 May;20(3):439-46.
41. Gartsman GM. Massive, irreparable tears of the rotator cuff. Results of operative debridement and subacromial decompression. *J Bone Joint Surg Am*. 1997 May;79(5):715-21.
42. Hansen ML, Otis JC, Johnson JS, Cordasco FA, Craig EV, Warren RF. Biomechanics of massive rotator cuff tears: implications for treatment. *J Bone Joint Surg Am*. 2008 Feb;90(2):316-25.
43. Clark J, Sidles JA, Matsen FA. The relationship of the glenohumeral joint capsule to the rotator cuff. *Clin Orthop Relat Res*. 1990 May;(254):29-34.
44. Rahu M, Kolts I, Põldoja E, Kask K. Rotator cuff tendon connections with the rotator cable. *Knee Surg Sports Traumatol Arthrosc*. 2017 Jul;25(7):2047-50.
45. Bey MJ, Song HK, Wehrli FW, Soslosky LJ. Intratendinous strain fields of the intact supraspinatus tendon: the effect of glenohumeral joint position and tendon region. *J Orthop Res*. 2002 Jul;20(4):869-74.
46. Mura N, O'Driscoll SW, Zobitz ME, Heers G, Jenken TR, Chou SM, Halder AM, An KN. The effect of infraspinatus disruption on glenohumeral torque and superior migration of the humeral head: a biomechanical study. *J Shoulder Elbow Surg*. 2003 Mar-Apr;12(2):179-84.
47. Arai R, Nimura A, Yamaguchi K, Yoshimura H, Sugaya H, Saji T, Matsuda S, Akita K. The anatomy of the coracohumeral ligament and its relation to the subscapularis muscle. *J Shoulder Elbow Surg*. 2014 Oct;23(10):1575-81.